Supporting Information

Shin and Mooney 10.1073/pnas.1611338113

SI Methods

Cell Lines and Reagents. Human myeloid leukemia cell lines (MOLM-14, U-937, and K-562) and a retroviral construct with *MLL-AF9* gene were kindly provided by the laboratory of David Scadden, Massachusetts General Hospital, Boston. These cell lines are also available from commercial vendors, such as American Type Culture Collection. Cells were cultured in RPMI, 1% penicillin and streptomycin, and 10% (vol/vol) FBS at 37 °C in 5% (or 50,000 ppm) CO_2. All drugs were obtained from LC chemicals except Cytarabine (Ara-C) from Sigma, Everolimus from Cell Signaling Technology, and MK-2206 from Biovision. All of the antibodies were purchased from Cell Signaling Technology. Phenol red-free DMEM (Fluorobrite) was purchased from Invitrogen.

Hydrogel Preparation and Mechanical Characterizations. Sodium alginate with a low molecular weight (LF10/60) was purchased from FMC Biopolymer and prepared as described previously (40). Briefly, alginate was dialyzed against deionized water for 3 d (molecular weight cutoff of 3,500 Da), filtered with activated charcoal, sterile-filtered, and lyophilized. It was then reconstituted in serum-free, phenol red-free DMEM at 4% (wt/vol) as a stock dilution. In some cases, an RGD peptide (GGGGRGDSP; Peptides International) was conjugated to alginate using carbodiimide chemistry at concentrations such that 5 or 20 RGD peptides were coupled to 1 alginate polymer on average. The coupling efficiency was previously characterized (40). The gels were formed by mixing alginate with different concentrations of calcium sulfate. The mechanical properties of alginate hydrogels were characterized with an AR-G2 stress-controlled rheometer (TA Instruments) by directly depositing them onto the surface plate of the rheometer. A 20-mm plate was brought down before the alginate started to gel, and the mechanical properties were then measured over time, with the storage modulus recorded at 0.5% strain and at 1 Hz. The storage modulus at these settings was measured to range from 25 to 1,000 Pa, which corresponds to Young's modulus ranging from 75 to 3,000 Pa, using the equations $E=2G(1+\upsilon)$ and $G=\sqrt{G'^2+G''^2}$, where E = Young's modulus, υ is Poisson's ratio of 0.5, G is the shear modulus, G' is the shear storage modulus, and G'' is the shear loss modulus.

Establishing Cell Lines That Express Exogenous Genes. To introduce mCherry and firefly luciferase in leukemia cells, lentiviral particles containing the vector with mCherry-IRES-firefly luciferase driven by the CMV promoter were purchased from the Vector Core at Massachusetts General Hospital. Cells were incubated with viral particles for 2 d. Single cells expressing mCherry were then sorted into 96-well plates via flow-activated cell sorting (FACS). Individual clones were expanded for 14 d. Clones were selected for further in vitro and in vivo analyses according to proliferation kinetics and intensity of fluorescence and luminescence signals. For *MLL-AF9* transduction, retroviral particles were obtained by co-transfecting the vector containing *MLL-AF9* or no gene ("empty") with the neomycin resistance gene and the packaging vector into Human Embryonic Kidney (HEK)-293 cells, followed by collection of supernatant at days 2–3 and ultracentrifugation through Amicon Ultra-15 (3-kDa cutoff ; Millipore) filters to concentrate particles. After introducing particles into leukemia cells, they were treated with G-418 (Invitrogen) to select for virally transduced cells. For *BCR-ABL* transduction, nerve growth factor receptor (NGFR) P210 (plasmid 27486) was a gift from Warren Pear, Addgene, Cambridge, MA, along with NGFR empty vector (plasmid 27489; Addgene) as previously published (41). Retroviral particles were obtained and used for transduction in a fashion similar to *MLL-AF9*. After transduction, NGFR-positive cells were sorted by FACS and expanded. The sorting and expansion cycle was repeated two to three times to achieve >95% of NGFR-positive cells for drug studies.

Tumor Growth Studies in Localized Xenograft Extramedullary Leukemia Models. All animal experiments were performed in compliance with NIH and institutional guidelines approved by the ethical committee from Harvard University. K-562 cells (10^6) expressing mCherry and firefly luciferase were encapsulated in a 5-mm diameter × 1-mm height alginate gel disk (~20 μL). A pair of gel discs with E = 100 or 3,000 Pa was s.c. implanted into each flank of 8- to 12-wk-old NOD/SCID/IL-2$\gamma^{-/-}$ mice. To monitor in vivo tumor growth over time, 3 mg D-luciferin was injected intraperitoneally into the 25-g mice followed by luminescence imaging with the IVIS Spectrum (PerkinElmer) within 30 min of injection. Average radiance (photons per second per centimeter squared per steradian) from each time point was measured from each implant for the first 3 wk. Beyond this time point, bioluminescence becomes saturated (Fig. S6*E*), and tumor volume was assessed using calipers by the modified ellipsoid formula: 1/2 × (length × width^2) (42).

Hierarchical Clustering Analysis. Before analysis, dose–response parameters, including IC_{50} and AUC values, of each drug from different stiffnesses were normalized against their respective values on plastic followed by log transformation. m values were not normalized. The complete linkage method with Euclidean distance measure was implemented using R (heatmap.2 function; https://www.r-project.org/) to perform hierarchical clustering of the dose–response data.

Intracellular Flow Cytometry. Cells were retrieved from cross-linked hydrogels by digesting with alginate lyase (3.4 mg/mL) for 15 min at 37 °C. Cell suspensions were then immediately fixed with 4% (wt/vol) paraformaldehyde for 10 min, followed by washing two times with PBS/0.1% BSA. Cells were then washed and resuspended in the staining media (PBS/0.1% saponin). Primary antibodies against total AKT and pAKT (Ser-473) were added to cells at 1:100 dilution along with Hoechst 33342 at 1:5,000 dilution. Cells were incubated at room temperature for 2 h. They were then washed with PBS and incubated with secondary antibodies (Alexa 647 anti-rabbit and Alexa 488 anti-mouse) for 30 min, followed by resuspension in PBS. Flow cytometry analysis was done using LSR II (BD).

Correlation Analysis. To observe relationships between Gompertz growth parameters and doses (normalized by IC_{50} values on plastic) in different matrix stiffnesses, Spearman correlation analyses were performed using GraphPad Prism 6. In some cases where cells were treated with higher drug doses the data could not be fitted to the Gompertz kinetics because cells did not proliferate significantly over time, and therefore they were excluded from correlation analysis. A correlation is considered statistically significant if $P < 0.05$.

Curve Fitting. The pharmacodynamics data were fitted to the logistical sigmoidal function

$$Y = Max + \frac{(Min - Max)}{1 + \left(\frac{IC_{50}}{X}\right)^m},$$

where Y is the cell number at dose X, Max and Min are the top and bottom asymptotes of the response, respectively, IC_{50} is the

concentration at half-maximal effect (potency), and m is the Hill slope. Constraints are $Min = 0$ (i.e., absolute IC_{50}) and $m > 0$. Area under dose–response curve (AUC) values were calculated over five doses using the trapezoid rule. Nonlinear least-squares regression was performed in GraphPad Prism 6. More than 90% of all of the dose–response data followed the sigmoidal model with $R^2 > 0.7$ and were used for further analyses.

Effects of matrix stiffening on AML cell number were fitted to the biphasic curve function

$$Y = Max + \frac{Init - Max}{1 + 10^{(\mathrm{Log}EC_{50} - E)\cdot m1}} + \frac{Final - Max}{1 + 10^{(E - \mathrm{Log}IC_{50})\cdot m2}},$$

Where Y is the cell number at stiffness X (log scale), *Init*, *Final*, and *Max* are the cell numbers at the initial, final, and maximum plateau phases, respectively, EC_{50} is the stiffness at half-maximal effect when cell number increases, IC_{50} is the stiffness at half-maximal effect when cell number decreases, and *m1* and *m2* are Hill slopes.

Cell Proliferation Kinetics Curve Fitting. The Gompertz function is defined as follows:

$$\frac{dN(t)}{dt} = K1 \cdot G(t) \cdot N(t)$$

$$\frac{dG(t)}{dt} = -K2 \cdot G(t),$$

where $N(t)$ is the cell number at time t, $K1{\cdot}G(t)$ is the growth rate at time t [i.e., $K1{\cdot}G(0)$ is the initial growth rate], and $K2$ is the deceleration rate. These differential equations can be solved analytically, resulting in the following equation:

$$N(t) = N(0) \cdot e^{\left(\frac{K1\cdot G(0)}{K2}\right)\cdot\left(1 - e^{-K2\cdot t}\right)}.$$

This equation was used to fit the cell proliferation kinetics data at different doses and different stiffnesses. Nonlinear least-squares regression was performed in GraphPad Prism 6. More than 70% of all of the proliferation kinetics data followed this model with $R^2 > 0.7$ and were used for further analyses.

Transforming $N(t)$ to the natural log scale will lead to the first-order growth kinetics equation:

$$\ln\left(\frac{N(t)}{N(0)}\right) = \frac{K1 \cdot G(0)}{K2} \cdot \left(1 - e^{-K2\cdot t}\right).$$

The log scale data from the in vivo tumor growth analysis for the first 3 wk were fit to this equation. For each fit, a Y-intercept was extrapolated, and each value was subtracted from the Y-intercept to correct for the background signal. Bioluminescence signals become saturated at week 4 (Fig. S6*E*), and hence the data beyond this time point were not used for fitting.

One way to compare luminescence signals between soft and stiff matrices is

$$Y = \frac{\ln(AX)}{\ln(X)} = \frac{\ln(A)}{\ln(X)} + 1,$$

where A is the fold difference in luminescence between soft and stiff, Y is the ratio between soft and stiff at the natural log scale, and X is the raw luminescence signal of the stiff matrix. Therefore,

$$A = e^{(Y-1)\ln(X)}.$$

For example, at week 2 when $X = 316.2$ and $Y = \sim 1.8$, A is ~100 (Fig. S6*C*).

Modeling an Autocrine Feedback Circuit of AML Cell Proliferation Modulated by Matrix Stiffening. We constructed a simple set of differential equations to describe an autocrine feedback circuit (Fig. 2 *B*, *i*) as follows:

$$\frac{dL}{dt} = \beta(E)L - \alpha(c)L \qquad \textbf{[S1]}$$

$$\frac{dc}{dt} = \delta(E)L - \gamma c, \qquad \textbf{[S2]}$$

where L is the number of leukemia cells at time t, c is the concentration of factors secreted from cells at time t, $\beta(E)$ is the rate of proliferation at matrix stiffness E, $\delta(E)$ is the rate of factor secretion at E, $\alpha(c)$ is the cell death rate at c, and γ is the factor degradation rate. These equations were solved computationally using MATLAB (MathWorks) with the function ode45 and the following values: $\gamma = 0.5$, $\alpha(c) = c$.

$$\beta(E) = \frac{m_\beta}{1 + \left(\frac{\beta E_{50}}{E}\right)^{k_\beta}}, \qquad \textbf{[S3]}$$

where βE_{50} is the E at half-maximal proliferation rate, m_β is the maximal proliferation rate, and k_β is the Hill coefficient of the proliferation rate.

$$\delta(E) = \frac{m_\delta}{1 + \left(\frac{\delta E_{50}}{E}\right)^{k_\delta}}, \qquad \textbf{[S4]}$$

where δE_{50} is the E at half-maximal factor secretion rate, m_δ is the maximal secretion rate, and k_δ is the Hill coefficient of the secretion rate.

To solve these equations analytically, at the steady state (ss), $dL/dt = 0$ and $dc/dt = 0$, and hence:

From Eq. **S1**:

$$\beta(E) = \alpha(c) = c_{ss}.$$

From Eq. **S2**:

$$\delta(E)L_{ss} = \gamma c_{ss}.$$

After substituting c_{ss} with $\beta(E)$,

$$\delta(E)L_{ss} = \gamma\beta(E)$$

$$L_{ss} = \frac{\gamma\beta(E)}{\delta(E)}$$

$$L_{ss} = \left(\frac{\gamma \cdot m_\beta}{m_\delta}\right)\frac{\left(1 + \left(\frac{\delta E_{50}}{E}\right)^{k_\delta}\right)}{\left(1 + \left(\frac{\beta E_{50}}{E}\right)^{k_\beta}\right)} = \left(\frac{\gamma \cdot m_\beta}{m_\delta}\right)\frac{E^{k_\beta}\left(E^{k_\delta} + \delta E_{50}{}^{k_\delta}\right)}{E^{k_\delta}\left(E^{k_\beta} + \beta E_{50}{}^{k_\beta}\right)}. \qquad \textbf{[S5]}$$

Plotting L_{ss} vs. E of Eq. **S5** with the initial $L_{ss} = 20$, $\gamma = 0.5$, $m_\beta = 10$, $m_\delta = 1$, $k_\beta = 2$, $k_\delta = 1$ shows

different biphasic curves with varied δE_{50} and βE_{50} as in Fig. 2*A*. Also, the equation suggests that the cell number will reach plateau with high E at

$$\lim_{E\to\infty} L_{ss} = \frac{\gamma \cdot m_\beta}{m_\delta}.$$

Analysis of an Alternative Model. Although the model in Fig. 2*A* considers when the proliferation rate is a function of matrix stiffness, and the death rate is a function of the secreted factors, it is possible that both proliferation and death rates directly depend on secreted factors as shown previously (21).

$$\frac{dL}{dt} = \beta(c)L - \alpha(c)L \quad \textbf{[S6]}$$

$$\frac{dc}{dt} = \delta(E)L - \gamma c \quad \textbf{[S7]}$$

$$\beta(c) = \frac{m_\beta}{1 + \left(\frac{\beta c_{50}}{c}\right)^{k_\beta}}, \quad \textbf{[S8]}$$

where βc_{50} is the c at half-maximal proliferation rate, m_β is the maximal proliferation rate, and k_β is the Hill coefficient of the proliferation rate.

$$\delta(E) = \frac{m_\delta}{1 + \left(\frac{\delta E_{50}}{E}\right)^{k_\delta}}, \quad \textbf{[S9]}$$

where δE_{50} is the E at half-maximal factor secretion rate, m_δ is the maximal secretion rate, and k_δ is the Hill coefficient of the secretion rate.

At the steady state (ss), $dL/dt = 0$ and $dc/dt = 0$:

From Eq. **S6**, given $\alpha(c) = c$:

$$\beta(c) = \alpha(c)$$

$$\frac{m_\beta}{1 + \left(\frac{\beta c_{50}}{c_{ss}}\right)^{k_\beta}} = c_{ss}. \quad \textbf{[S10]}$$

This suggests that c_{ss} is independent of L or E.

As in Eq. **S5**, consider the case when $m_\beta = 10$ and $k_\beta = 2$. Rearranging Eq. **S10** leads to a quadratic equation:

$$c_{ss}{}^2 - 10c + \beta c_{50}{}^2 = 0. \quad \textbf{[S11]}$$

Solving Eq. S11 leads to

$$c_{ss} = 5 - \sqrt{25 - \beta c_{50}{}^2}\,. \quad \textbf{[S12]}$$

Because $25 - \beta c_{50}{}^2 \geq 0$,

$$0 \leq c_{ss} \leq 5.$$

From Eq. **S7**, given $\gamma = 0.5$:

$$L_{ss} = \frac{0.5c_{ss}}{\delta(E)} = \frac{0.5c_{ss}}{m_\delta}\left(1 + \left(\frac{\delta E_{50}}{E}\right)^{k_\delta}\right). \quad \textbf{[S13]}$$

For a biphasic "concave-down" curve to exist there has to be a plateau at some value of E above zero. In other words,

$$\frac{dL_{ss}}{dE} = 0 \text{ when } E > 0.$$

However,

$$\frac{dL_{ss}}{dE} = -k_\delta \frac{0.5c_{ss}}{m_\delta} \delta {E_{50}}^{k_\delta} E^{-k_\delta - 1} = 0.$$

The only solution is $E = 0$ when $k_\delta < -1$. No solution exists when $k_\delta \geq -1$ ($k_\delta \neq 0$). Hence, no biphasic relationship between cell number and matrix stiffness is observed at the steady state in this case.

Network Analysis of Signaling Pathways. A physical interaction network consisting of drug targets ("nodes") in this study was constructed using Cytoscape, open-source software for network analysis (43). The physical interaction data were derived from multiple databases through the software, including BioGrid and MiMI. The results from previous tandem affinity purification and immunoprecipitation experiments with human cells were used for analysis. The results were filtered further based on previously reported confidence scores (>0.3 out of 1.0) for each interaction that were computed from the number of interactions and type of experiment, and the number of citations provided for each interaction. The total of 19 nodes and 41 interactions were used to construct the network. The interactions were then clustered on the basis of network topology or "interconnectedness" by using the clusterMaker2 plugin and the GLay Community Clustering algorithm, which identifies heavily connected subclusters via iterative removal of edges from the network. Three distinct clusters were identified and plotted in the interaction map. Arrows were assigned based on established knowledge on AKT and MAPK pathways. Interactions within the same cluster were colored black, and those in different clusters were colored gray.

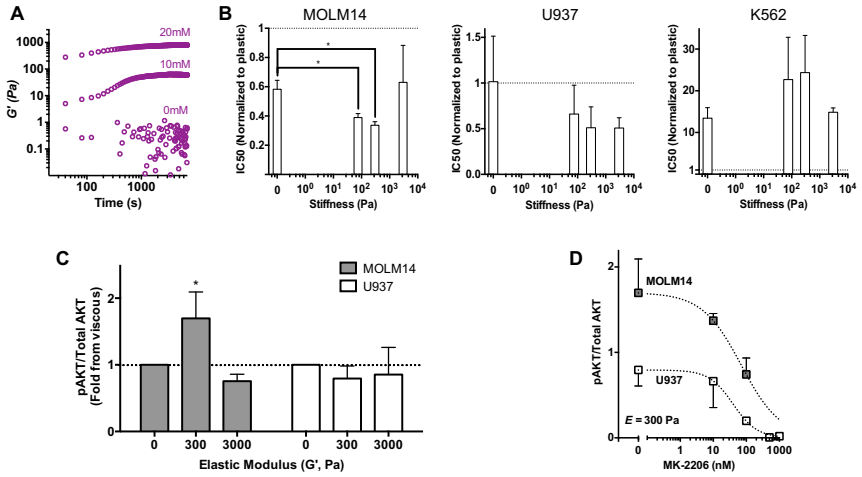

Fig. S1. (*A*) Mechanical characterization of alginate hydrogels formed by different calcium concentrations (millimolar) during gelation. G′ (pascals) is the shear storage modulus. (*B*) IC_{50} values for inhibition of cell proliferation across matrix stiffness by MK-2206. The IC_{50} values were normalized against corresponding values on plastic. Error bars indicate ± SEM, $n = 3$ experiments, $^*P < 0.05$ from one-way ANOVA with Tukey's HSD test (relative to 0 Pa). (*C*) Levels of pAKT in myeloid leukemia cells across matrix stiffness were evaluated by intracellular flow cytometry. $^*P < 0.01$ from one-way ANOVA with Tukey's HSD test (relative to 0 Pa). (*D*) Dose–response curves of pAKT inhibition by MK-2206 in leukemia cells encapsulated in 300-Pa gels. pAKT was measured by intracellular flow cytometry. Values normalized to pAKT of cells in untreated 0 Pa.

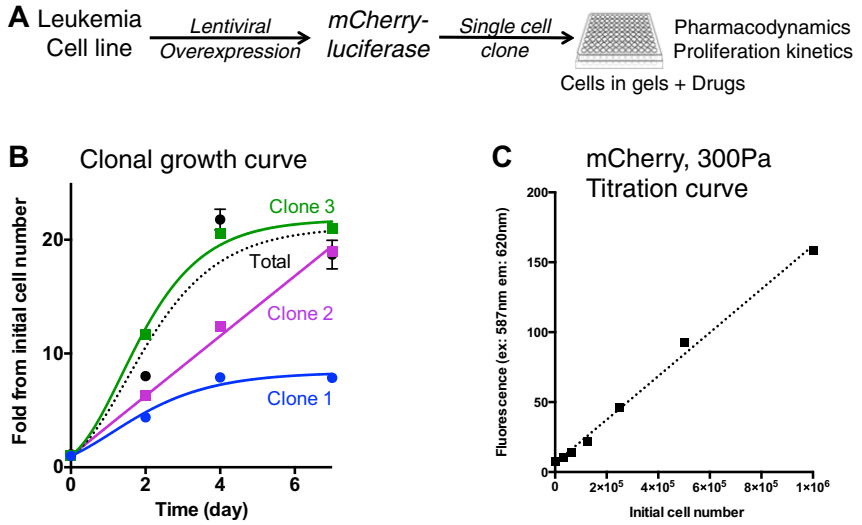

Fig. S2. Developing a screen to quantify proliferation and pharmacodynamics. (*A*) An overview of the screen approach. Cells were transduced with mCherry-luciferase by lentivirus followed by single-cell mCherry positive clone selection, expansion, encapsulation of cells in gels, and deposition in a 96-well. Cell proliferation kinetics in the presence of different drugs was then evaluated by fluorescence. (*B*) Cell proliferation kinetics of select mCherry-positive K-562 clones. (*C*) The graph showing mCherry fluorescence vs. cell number of clone 3 cells encapsulated in 300-Pa gels. Linear fit $R^2 > 0.95$.

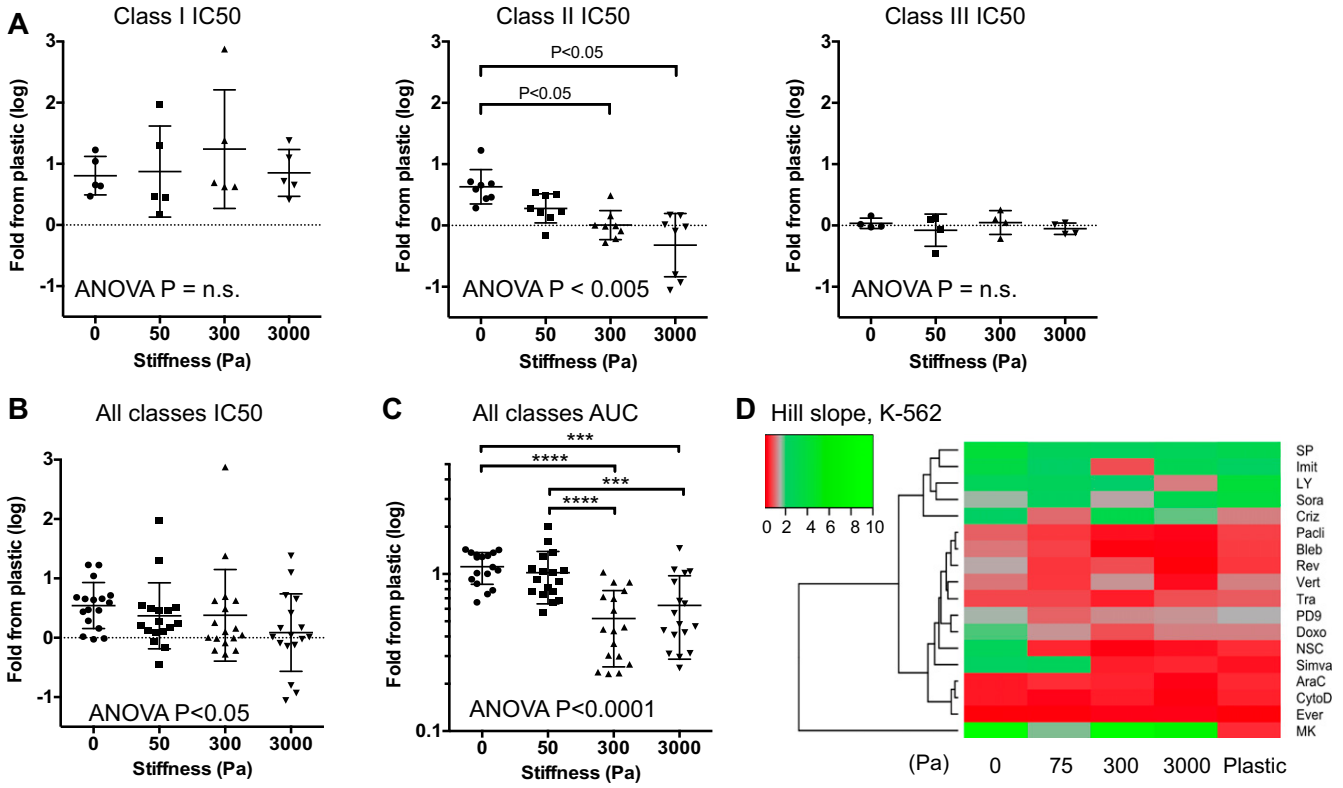

Fig. S3. (*A*) IC_{50} values of drugs from each drug class. For class II, one-way ANOVA $P < 0.005$, Tukey's HSD test $P < 0.05$, correlation analysis $P < 0.0001$. (*B*) IC_{50} values of drugs from all of the classes against K-562 cells across matrix mechanics. One-way ANOVA $P < 0.05$, followed by Tukey's HSD test. (*C*) AUC values of dose–response curves across matrix mechanics for K-562 cells. One-way ANOVA $P < 0.0001$, Tukey's HSD test ***$P < 0.005$, ****$P < 0.001$. In all graphs, values normalized to tissue culture plastic. (*D*) Clustering analysis of Hill slope values from individual drugs tested against K-562 cells.

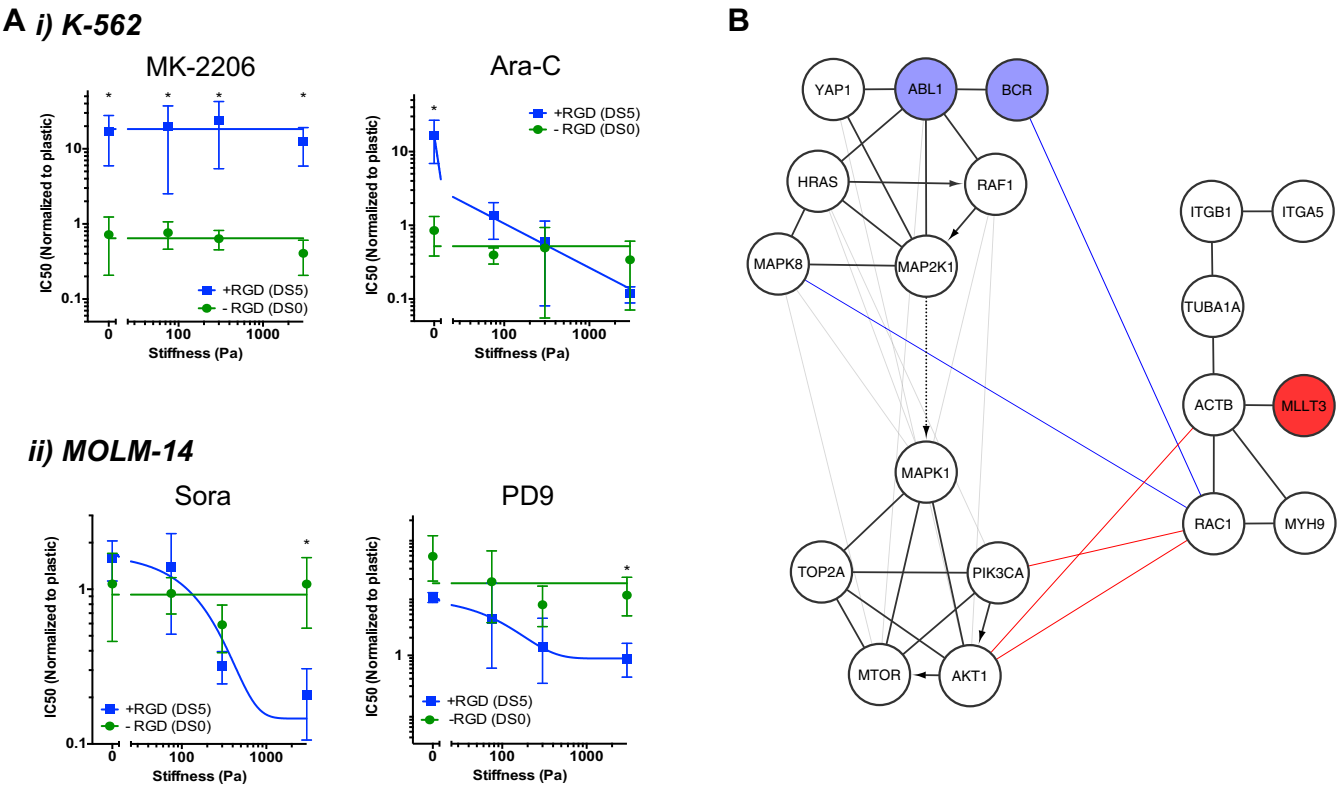

Fig. S4. (*A*) Drug resistance to class I and II drugs for K-562 (*i*) and MOLM-14 (*ii*) is integrin ligand-dependent. IC_{50} values derived from cells in hydrogels with (DS = 5) or without RGD were normalized against plastic and plotted across different mechanics. Error bars indicate ± SEM, $n = 3$ experiments, $^*P < 0.05$, paired *t* test. (*B*) Computational construction of a physical interaction network (*SI Methods*) reveals that proteins from protooncogenes of leukemias interact with distinct signaling clusters.

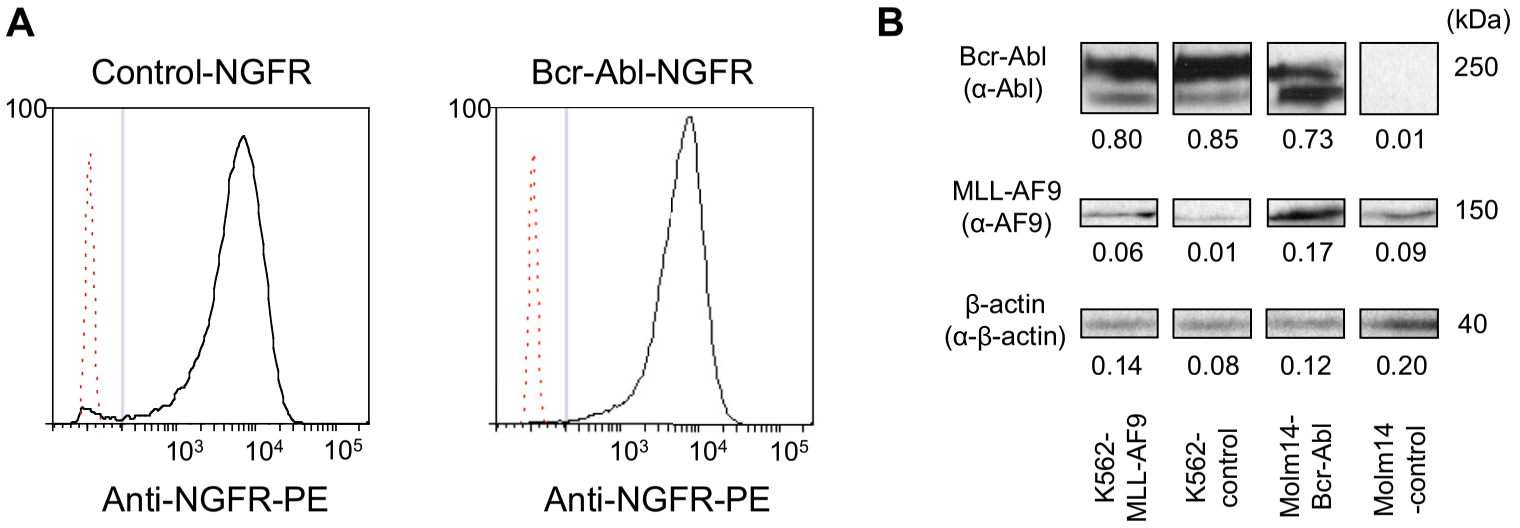

Fig. S5. (*A*) Transduction of MOLM-14 cells with a retroviral vector containing empty (*Left*) or Bcr-Abl (*Right*) confirmed by flow cytometry analysis. A truncated form of NGFR was used as a reporter to both sort transduced cells using FACS and confirm transduction efficiency using flow cytometry. A red dotted line in the flow cytometry plots indicates cells that are not transduced with a NGFR vector. (*B*) Protein expression of Bcr-Abl and MLL-AF9 in cells by Western blot.

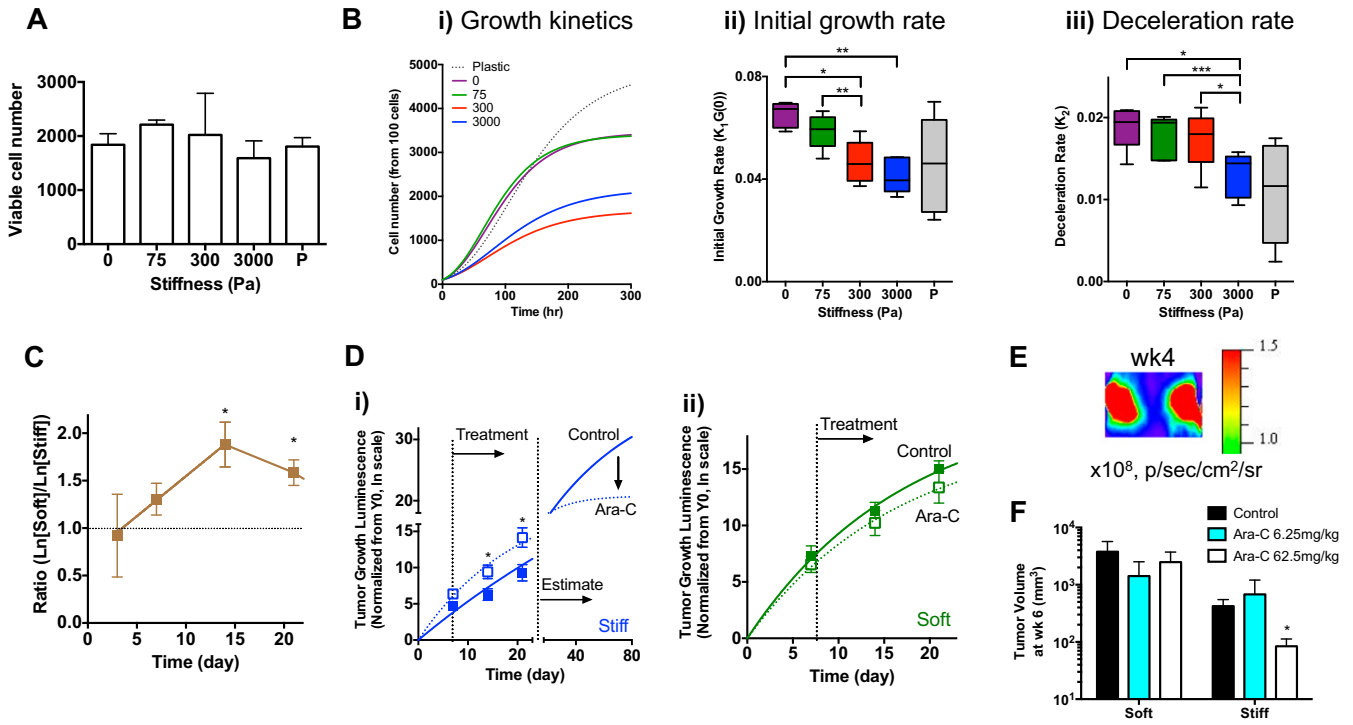

Fig. S6. (*A*) The number of viable cells after cell encapsulation in gels at day 0. (*B*) Slow but sustained growth of K-562 cells upon matrix stiffening. Matrix stiffness influences parameters of proliferation kinetics of K-562 cells. (*i*) Representative Gompertz curve fits (*SI Methods*) over 2 wk. (*ii*) Initial growth rate. (*iii*) Deceleration rate. For *ii* and *iii*, one-way ANOVA $P < 0.05$ with Tukey's HSD test, $*P < 0.05$, $**P < 0.01$, $***P < 0.005$. (*C*) K-562 cells in soft matrix show enhanced tumor growth compared with stiff matrix after s.c. implantation in vivo. Average radiance data from soft and stiff were converted to the natural log scale and divided (*SI Methods*). Straight line fit between day 3–14: $Y = 0.084t + 0.70$ (t: day). Data from $n = 15$ mice from three independent experiments. Paired *t* test, $*P < 0.005$. Error bars indicate ± SEM. (*D*) Tumor growth kinetics with Ara-C. (Plateau, acceleration rate) from the first-order kinetics fit for (*i*) stiff untreated (40, 0.56), Ara-C (20.8, 0.84) and (*ii*) soft untreated (22.5, 1.17), Ara-C (17.7, 1.15). Data from $n = 8$ mice from two independent experiments. Paired *t* test $*P < 0.05$. Error bars indicate ± SEM. (*E*) Bioluminescence signals become saturated at week 4. The same scale as in Fig. 4*A* was used. (*F*) Tumor volume at week 6 after implantation with different doses of Ara-C. Data from $n = 5$ mice for each group from two independent experiments. One-way ANOVA with Tukey's HSD test $*P < 0.05$ control vs. 62.5mg/kg Ara-C. Error bars indicate ± SEM.

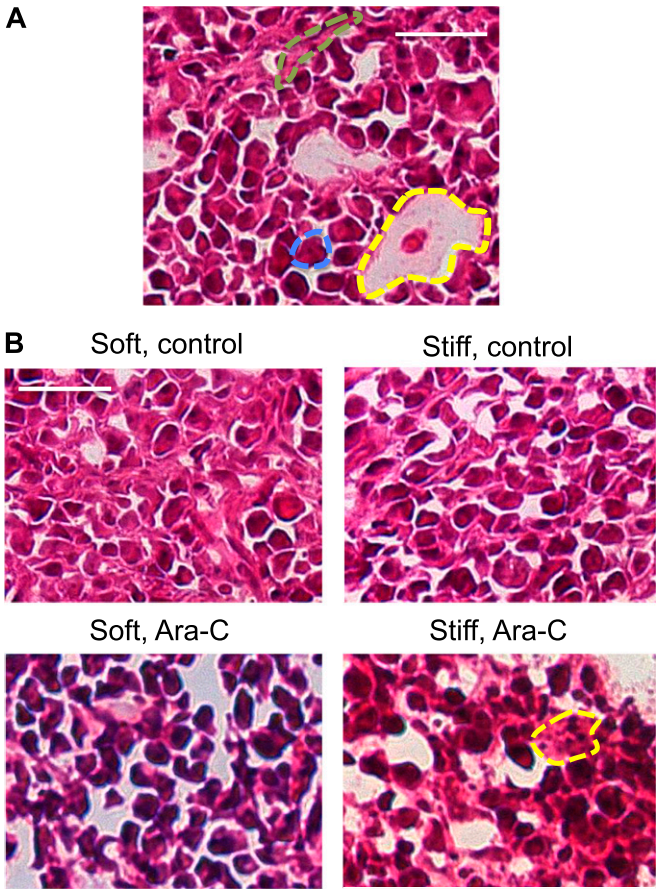

Fig. S7. Histological sections from s.c. implanted K-562 cells stained with hematoxylin and eosin. (*A*) A representative image showing blood cells (blue), stromal-like cells (green), and hydrogel fragments (yellow) after 2 wk of tumor implantation. (*B*) Representative images showing general morphological features of different treatment groups. Yellow: A region with nuclear fragments. (Scale bars: 50 μm.)

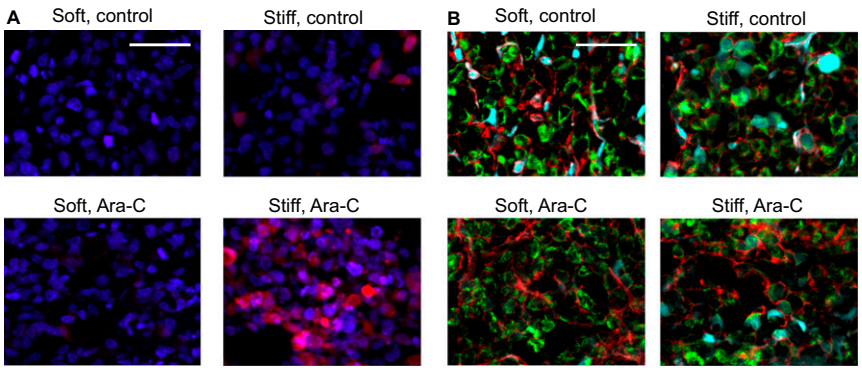

Fig. S8. Immunofluorescence staining of histological sections from s.c. implanted K-562 cells. (*A*) Representative images showing nuclei (blue) and cleaved caspase-3 (red). (Scale bar: 50 μm.) (*B*) Representative images showing F-actin (red), human mitochondria (green), and YAP (cyan). (Scale bars: 50 μm.)

Table S1. List of tested drugs and dose ranges

Drug	Abbreviation	Pathway	Tested dose range, nM
Everolimus	Ever	mTOR	0.1–1,000
MK-2206	MK	Akt	10–50,000
Doxorubucin	Doxo	DNA topoisomerase 2 (TOP2)	0.1–100
Crizotinib	Criz	c-MET kinase	0.1–1,000
Verteporfin	Vert	YAP/TAZ	10–2,000
Imitinib	Imit	ABL/KIT	0.1–100
Trametinib	Tra	MEK	0.1–100
NSC23766	NSC	Rac	100–50,000
Reversine	Rev	MEK, myosin-II	10–5,000
Paclitaxil	Pacli	Microtubule	10–1,000
Cytarabine	AraC	DNA synthesis	1–100
Blebbistatin	Bleb	Myosin-II	1,000–20,000
Simvastatin	Simva	Cholesterol	100–50,000
Sorafenib	Sora	RAF	100–5,000
SP600125	SP	JNK	5,000–40,000
PD98059	PD9	MAPK/ERK	10–50,000
Fasudil		Rho-kinase	300–20,000
Ruxolitinib		JAK	10–10,000